IEEE/CSC & ESAS European Superconductivity News Forum (ESNF), No. 15, January 2010
Published in Supercond. Sci. Technol. (SuST) **23** (2010) 124001 (7pp)

Materials process and machine application of bulk HTS

M. Miki[1, 2], B. Felder[1], K.Tsuzuki[1], Y. Xu[1], Z. Deng[1], M. Izumi[1], H. Hayakawa[2], M. Morita[3] and H. Teshima[3]

[1] Department of Marine Electronics and Mechanical Engineering, Tokyo University of Marine Science and Technology, 2-1-6, Etchu-jima, Koto-ku, Tokyo 135-8533, Japan.

[2] Kitano Seiki Co. Ltd., 7-17-3, Chuo, Ohta-ku, Tokyo 143-0024, Japan.

[3]Nippon Steel Co. Ltd., 20-1, Shintomi, Huttsu-shi, Chiba 293-8511, Japan.

E-mail: d082025@kaiyodai.ac.jp

Abstract

We report the completion of a refrigeration system for rotating machines associated with the enhancement of the trapped magnetic flux of bulk high-temperature superconductor (HTS) field poles. A novel cryogenic system was designed and fabricated. It is composed of a low loss rotary-joint connecting a closed-cycle thermosyphon under a GM cryocooler and the rotor by using a refrigerant. Condensed neon gas was adopted as a suitable cryogen for the operation of HTS rotating machines with field poles composed of RE-Ba-Cu-O family materials, where RE is a rare-earth metal. As for the material process of the bulks HTS, thanks to the magnetic particle addition to $GdBa_2Cu_3O_{7-d}$ (Gd123) bulk superconductors, more than 20 % increase of the trapped magnetic flux density was achieved at liquid nitrogen temperature. The field pole Gd123 bulks up to 46 mm in diameter were synthesized with an addition of Fe-B alloy magnetic particles and assembled into the testing synchronous machine rotor. Successful cooling of the magnetized rotor field poles down to 35 K and the first-step low-output-power rotating operation was achieved up to 720 rpm in the test machine with eight field-pole bulks. Present results submit a substantial basis for the completion of a prototype system of the rotating machinery of applied HTS bulks.

Keywords: AC losses, flux pinning, Gd-Ba-Cu-O bulk superconductors, magnetic particles, neon, pulsed-field magnetization, thermosyphon

1. Introduction

Large-scale single melt-growth bulk high-temperature superconductor (HTS), able to trap magnetic flux, attract much interest for potential applications to synchronous rotating machines such as motors, generators, MAGLEV, MRI [1-3]. The bulk-HTS magnets enable us to maintain a high magnetic flux density up to 17 T at low temperature upon magnetization below the superconducting transition temperature. Upon magnetization, penetrated flux is possibly captured around specific material structures such as defects, non-superconducting portions and some other parts in which the free energy required by the flux to stay is lower than in the superconducting phase. The particles able to pin flux are called pinning centers. An optimized flux trapping provides a highly concentrated magnetic flux

and thus a high electromagnetic force around the field poles. Another aspect is the magnetization process. These magnets can be excited without the presence of high electric current cables/leads. These advantages lead to a simple structure, light-weight body and high redundancy. The bulk HTS materials are mostly made from the RE-Ba-Cu-O family and have an equivalent crystal structure with the so-called 2G [4] wire materials. Therefore, they are highly promising materials and magnets to be practically used in a temperature range of 65 K to 30 K.

In our laboratory, we have developed an axial gap-type synchronous motor with Gd-123 bulk-HTS magnets for a low-speed propulsion system since 2001. Two different types of motors have been mechanically designed, constructed and studied continuously. They have been designed for 30 kW and 100 kW classes and have been tested at 10 kW, with single rotor, and 16 kW, with twinned rotor. Both those outputs were achieved with an operation under liquid nitrogen [5, 6].

Presently, in order to approach the designed specifications, we have completed a couple of tasks concerning materials and machinery, as the following activities. First, we succeeded in the improvement of the magnetic flux trapping function of the bulk $GdBa_2Cu_3O_{7-d}$ (Gd123). Gd123 provided advantages on flux pinning for critical current density J_c under magnetic field and is now tested and under study for wire production [7]. According to the preliminary study by Xu et al. [8], the addition of soft-magnetic particles was applied to increase the critical current J_c. Secondly, we adopted neon gas as a cryogen to cool down and keep a stable operation of rotating machines as well as bulk-HTS magnets.

2. Material process of bulk HTS and peripheries

2.1. Improvement of the HTS magnet

Figure 1 shows the critical current density J_c as a function of the magnetic field in the melt-growth single domain Gd-Ba-Cu-O bulks fabricated in air with and without soft-magnetic Fe-B-Si-Nb-Cr-Cu alloy particles addition [9]. These magnetic alloy particles are commercially available from Hitachi Metals with the product name of FINEMET [10]. We abbreviate these soft-magnetic particles as MP in the following paper. Thanks to the MP addition of 0.4 mol%, Fig. 1(a) illustrates the enhancement of the J_c in a range up to 4 T, in the specimen taken from just under the seed crystal placed at the center of the top surface during melt-growth process [9]. Similar J_c enhancement has been observed in the sample cut from the growth sector 1 mm under the surface and 4 mm away from the seeding center as shown in Fig. 1. To realize a high torque density in the rotational machinery, the bulk HTS field pole needs to possess a large capability of trapped flux. In order to enhance the trapped flux, the J_c has to be crucially enhanced. The introduction of artificial pinning centers is known as one of the effective methods to provide a crucial enhancement of the J_c [11]. Thus, in the previous work, the soft-magnetic alloy particles were introduced in the bulk HTS. This result revealed that the J_c of Gd-Ba-Cu-O bulks fabricated in air were potentially improved by introduction of magnetic particles [8].

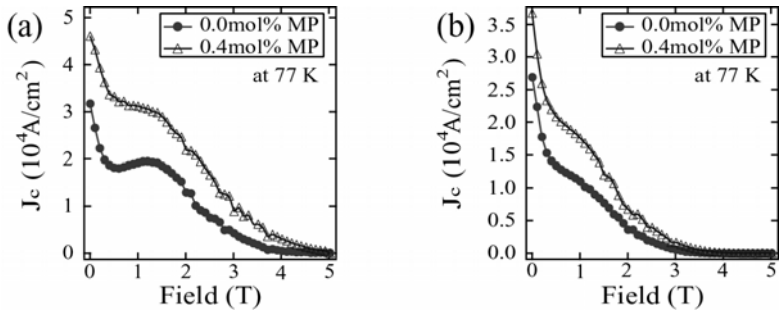

Figure 1. Critical current density of the bulk with and without 0.4 mol% Fe-B-Si-Nb-Cr-Cu (MP) addition measured by SQUID (a) the J_c in a range up to 4 T in the specimen taken from 1 mm under the seed crystal placed at the center of the top surface during melt-growth process [9]. The applied magnetic field H is parallel to the c-axis, (b) the J_c as a function of the applied field in the sample cut from the growth sector 1 mm under the surface and 4 mm away from the seeding center, as shown in Fig. 2. The applied magnetic field H is parallel to the c-axis.

From the results in Sec. *2.1* and Fig. 1, we have prepared a Gd123 puck, 46 mm in diameter, in accordance with a practical assembly into the rotor as a field pole. Precursor powders with the nominal composition of Gd-123 + 40 mol% Gd-211 + X mol% MP, where X = 0.0, 0.4 were mixed. 10 wt% of Ag and 0.5 wt% of Pt were added and mixed together. Those pellets were heated following a certain temperature program to perform hot-seeding melt-process and finally they were annealed in oxygen.

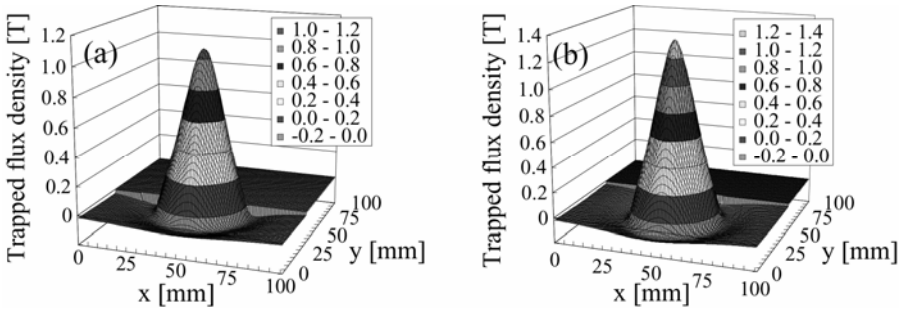

Figure 2. Trapped flux distribution of Gd-Ba-Cu-O bulks, 46 mm in diameter, at the liquid nitrogen temperature, (a) without MP addition (b) with 0.4 mol % MP addition.

Figure 2 shows the trapped field distributions of the bulks (a) without magnetic particle addition, (b) with 0.4 mol% MP. The trapped field experiments were conducted at the liquid nitrogen temperature by a field-cooling process with an applied field of 3.5 T.
The single-grain bulk with 0.4 mol % MP exhibits a trapped field of 1.34 T, which is 25 % larger than the sample without addition of MP. The bulk with MP addition recorded 646 μWb as the integrated flux, which represents a 17 % enhancement of the flux compared to the bulk without addition. These results revealed that the trapped flux properties of Gd-Ba-Cu-O bulks were potentially improved by the introduction of MP particles.

2.2. Optimization of the cooling system for magnetization of HTS

The optimization of our cooling system has gone through a number of evolution steps which are described in the following paragraph. Typically, the T_c of HTS bulks are higher than the liquid nitrogen temperature, e.g. 92 K in the case of Gd bulks. Hence, liquid nitrogen is a very convenient refrigerant to use, which we therefore first adopted as the cryogen for our prototype motor. The circulation of nitrogen does not require any complicated device and allows a quick cooling of the field poles.
The critical current of superconductor increases when decreasing the temperature and liquid nitrogen does not allow temperatures lower than 77 K. That is why we then changed the cryogen from liquid nitrogen to liquefied neon gas by using a closed-cycle thermosyphon. We successfully cooled down the bulks to a temperature of 38 K in 2007 [12].
In order to enhance the efficiency and the overall cooling power, meaning the increase of the maximum allowable heat load coming to the rotor, we modified and optimized this cooling system, especially the condenser part. Then, to decrease the cooling down time and enhance the temperature stability of the bulks under operation, we optimized the parameters of the cooling, such as the quantity and/or the pressure of neon.
More concretely, the Gifford-McMahon type cryocooler has not changed (Cryomech AL330 running at 50 Hz) but the condenser to which it is attached has seen several modifications through the years. The first version was merely a pipe in which the neon gas was flowing, winded around the cold head. But we were having a hard time controlling the temperature and the small diameter of the pipe was causing problems with the unwanted freezing of neon.
The pipe-type condenser was changed for a more conventional condensation chamber, whose upper part is fixed to the cold head by the intermediary of a plate in which is located a heater for temperature control. The all-stainless design was very basic but the choice of the material was not appropriate, considering the need of a high thermal conductivity, and the heat exchange surface was quite small. It led to a usable thermosyphon, yet the cooling times were too long, leading us to modify the inner

structure of the condensation chamber again in 2009.
The condenser currently in use is now made of OFHC (Oxygen Free High thermal Conductivity) copper for all heat conductive parts. We also replaced the upper plate of the condensation chamber by a trapezoidal-shape eleven-fin array, shown in figure 3 (a), whose dimensions were calculated and optimized for neon use. The transportable heat has now theoretically increased above 750 W. The disposition of the cold head over the fin array is displayed in figure 3 (b).
We also developed an appropriate answer to another challenging problem in the operation of superconducting machines. This vital part is a compact and light-weight rotating joint between the static cooling system and the rotating cryostat, named cryo-rotary joint (cryo-RJ), and was developed in our laboratory in 2008 [13, 14]. Basically composed of a multi-layer vacuum insulation and of two magnetic fluid seals, it allows a smooth rotation in a large range of rotating speeds and represents a heat invasion of less than 4 W.

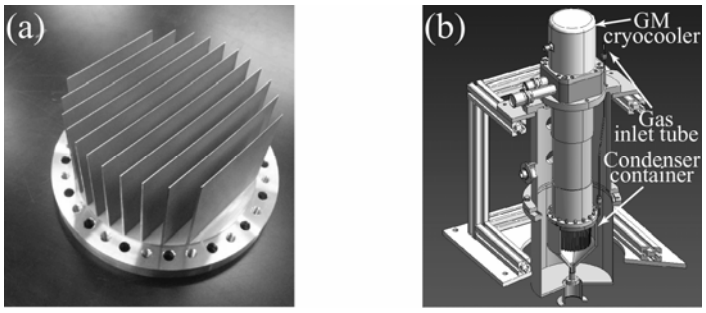

Figure 3. (a) Manufactured fin array. (b) Schematic view of the modified condenser system.

3. Machine application of HTS for rotating machine

3.1. Field-pole magnets

For this present study, we prepared 3 different bulks for field-pole magnets: 1) two kinds of MP-doped bulks with different compositions, 2) five double-stacked bulks composed of 2 different bulks bonded together with a voluntary mismatch of the growth-sector boundaries [15], 3) a normal single domain bulk. The details of each bulk are listed in Table 1.

Table 1. Characteristics of field-pole Gd123 bulk magnets.

Sample	Diameter [mm]	Thickness [mm]	Note
A	46	15	Gd123 + 40mol%Gd211 + **1.0mol%MP** + 52.5mol%Pt + 1.9mol%Ag2O
B	60	20	Double-stacked bulk [15]
C	60	20	Double-stacked bulk
D	60	20	Normal single domain bulk
E	46	15	Gd123 + 40mol%Gd211 + **0.4mol%MP** + 52.5mol%Pt + 1.9mol%Ag2O
F	60	20	Double-stacked bulk
G	60	20	Double-stacked bulk
H	60	20	Double-stacked bulk

Two types of Hall sensors and thermocouples were employed to detect the trapped magnetic flux and the temperature of the bulks on the rotor. BHT-921 Hall sensors (F.W.BELL from the U.S.) and THS-118 Hall sensors (Toshiba from Japan) were located 2 mm over the surface of the bulks. 5 pairs of normal-Silver versus Au-0.07 % Fe thermocouples (TC) were attached on the bulks surfaces. Figure 4 (a) and (b) represent the positions of the bulks and sensors, respectively.

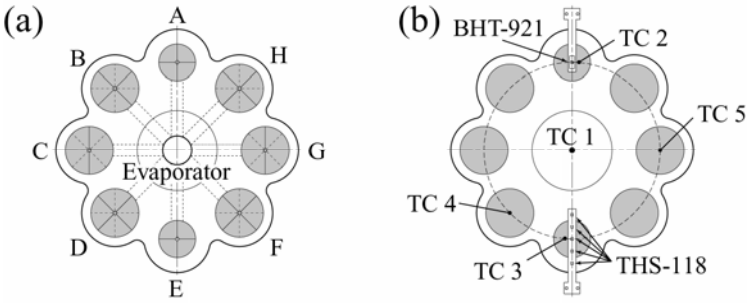

Figure 4. (a) Positions of the Gd123 bulk HTS field poles on the rotor plate. Dashed lines from the evaporator center to the bulk field poles indicate the assembly of copper bars for conduction cooling between the evaporator and each bulk field pole. (b) Positions of the Hall sensors and thermocouples. The dashed circle represents the trajectory along the point by point measurements during synchronous rotation of the motor.

The bulk-HTS magnets and the evaporator were connected with copper plates for conduction cooling.

3.2. Experimental apparatus for the operation of the bulk HTS synchronous motor

The test apparatus was composed of 5 major elements: the cooling system, the bulk HTS synchronous motor, the magnetizer, the inverter for rotation and the data acquisition system, as displayed in figure 5.

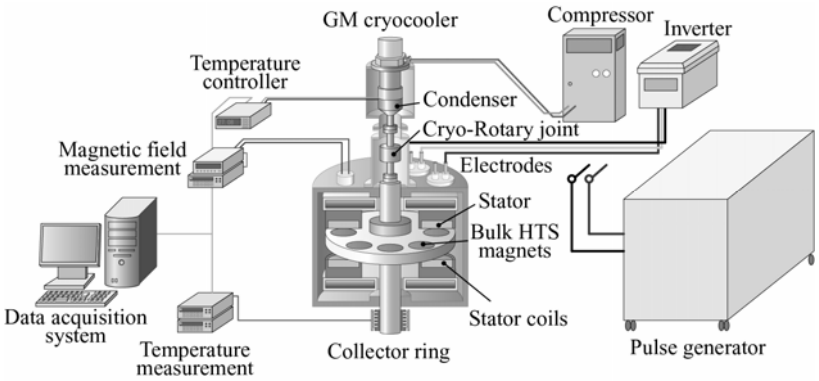

Figure 5. Schematic view of the bulk HTS synchronous motor and the peripheral systems.

The thermosyphon cooling system was connected to the rotor of the motor through the cryo-RJ which allows a smooth rotation and stable cooling. The stator coils played the role of both magnetizing coils and electrodes; therefore the pulse generator and inverter were switched depending on the situation.

3.3. Magnetization in the motor

Pulsed-field magnetization (PFM) was employed to magnetize the Gd123 field-pole magnets. Split-type stator coils shown in figure 6 play the role of magnetization coils with a pulsed dc current [4]. During the magnetization, a bulk-HTS magnet is placed between a pair of stator coils i.e., the magnetizing coils as shown in figure 6 (a) and 6 (b), schematically. In the previous study, we have proposed a magnetization technique which was named Controlled Magnetic field Distribution Coil (CMD-C) method [16]. The application of the CMD-C enables us to obtain a cone-shape distribution of the trapped magnetic flux density under PFM [16]. Figure 6 shows a schematic view and the principle of the CMD-C.

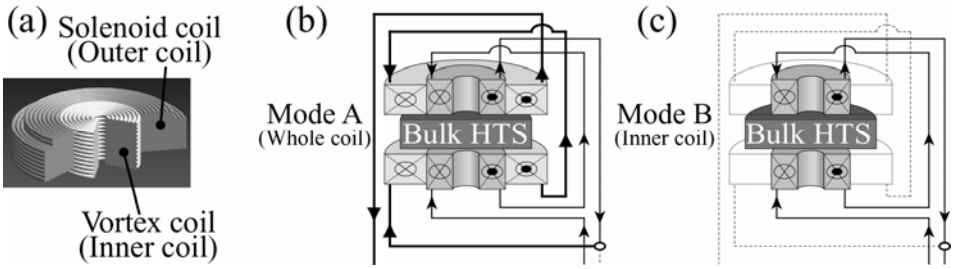

Figure 6. (a) Structure of the CMD-C, composed of an outer solenoid coil and an inner vortex coil. (b) In the case of mode A, outer and inner coils were connected in series. (c) In the case of mode B, only the inner coil was excited.

During the magnetization, the temperature of the magnetizing coils was kept around 100 K by using liquid nitrogen to generate a high magnetic field with a very high, usually 2 kA to 4 kA, pulse current.

3.4. Synchronous operation

To investigate the influence of the AC losses, we carried out the synchronous operation tests by applying an AC external magnetic field coming from the stator coils. A 300-minute synchronous operation test was carried out. The details of the operating conditions are as follows: 1) 50 rpm / 60-minute operation, 2) 300 rpm / 60-minute operation and 3) 50 rpm / 300 minutes.

4. Cooling and operation of the HTS motor

4.1. Verification of the cooling

A comparison of the cooling times for the different cryogens and devices we used is presented in the figure 7. In the previous works, the bulk-HTS magnets were cooled down below 85 K with circulated liquid nitrogen. This difference in temperature between the temperatures of the cryogen and of the bulks may be explained by heat radiation coming from the armature coils to black-body HTS bulks. As shown in Fig. 7, the cooling time from the room temperature was very rapid but involved the constant feeding of liquid nitrogen.

When we changed the cryogen from liquid nitrogen to condensed neon by the use of a closed-cycle thermosyphon, the temperature of the bulks reached about 38 K. However, more than 2,000 minutes were necessary to cool down the bulks due to the basic all-stainless cooling system design described in a previous section. The main target of drastically decreasing the temperature for trapping a higher flux was yet already reached.

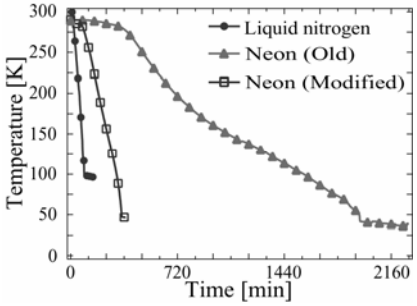

Figure 7. Comparison of the cooling times as a function of the modifications.

Finally, the recently optimized condenser allowed us to reach the same range of temperatures, but with a cooling time divided by six when following the suitable parameters. This cooling time of 340 minutes has become the new reference in cooling time of the eight HTS bulks comprised in our

prototype motor.

4.2. Magnetization of the field-pole Gd123 bulks on the rotor

To evaluate the effect of MP doping, we performed the PFM experiment inside the motor. The CMD-C method was used for this experiment to achieve cone-like flux density distributions of the trapped fields. The parameters of the PFM were determined in reference to the previous works and those values are shown in table 2.

Table 2. Parameters of the PFM. The coil modes are as explained in figure 6.

Number of pulses	Bulk temperature [K]	Applied field [T]	Coil mode
1st	70	6	A
2nd	70	7	A
3rd	65	8	B
4th	65	9	B

Now, the principle of the CMD-C should be explained again. When we use the coils for which the diameter is larger than those of the bulks, a high integrated flux is trapped, but the trapped-field distribution is likely to be inhomogeneous. On the other hand, when we use the coils with a smaller diameter than those of the bulks, the flux density distribution becomes homogeneous like a cone.

After magnetization, the maximum trapped magnetic field densities of normal single-domain (bulk D) and MP-doped bulks (Bulk E) were 0.43T and 0.42 T, respectively. The measured trapped magnetic fields along the central measurement trajectory were normalized to compare the different-size bulks. In detail, we integrated the measured value and divided by the scanning area of the Hall sensor. The calculated values of both bulk D and E as a function of the number of pulses are shown in figure 8.

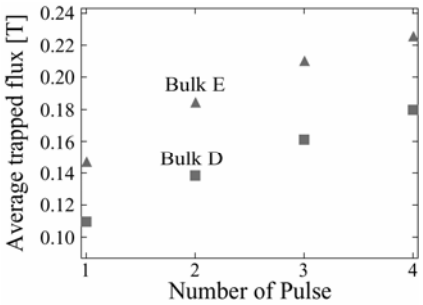

Figure 8. Representative comparison of the trapped magnetic flux between bulk D (normal) and bulk E (MP-doped).

According to the figure 8, the trapped magnetic flux of the MP-doped bulk was 1.1 to 1.4 times higher than the normal ones', which is in good agreement with the results in the preceding report studied under field-cooling magnetization [17]. Thus, the effect of the MP addition on flux trapping was practically verified under PFM inside the motor. These results were verified with the measurements of all the magnetized bulks but for clarity reasons, only these two bulks are shown for comparison.

4.3. Observation of the flux creep

The flux creep is one of the important parameters when we apply bulks as field-pole magnets. Hence, we measured the initial creep of the trapped magnetic flux with and without MP doping. In this experiment, we magnetized by using PFM with CMD-C, but the parameters were different from those used in the section 4.2. The bulks were cooled down to about 40 K immediately after PFM.

The trapped magnetic field was measured by a 1-degree-step rotation of the rotor by using Hall sensors which were placed as shown in Fig. 4 (b). The measurement times were just after, 30 and 90

minutes after PFM. The maximum trapped magnetic fields of bulks D and E were 0.61 T and 0.44 T, respectively. Figure 9 shows the average trapped flux as a function of time after the magnetization. The calculation of the averaged value was obtained with the method shown in section 4.2.

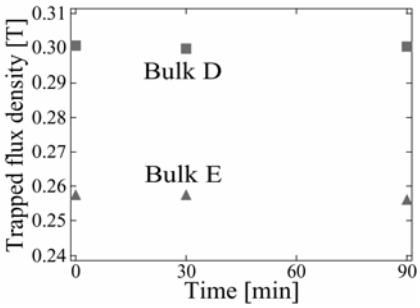

Figure 9. Evolution of the average trapped flux after magnetization

The values of initial creep of bulks D and E, -0.1 % and -0.55 %, respectively, were quite small compared with the previous study [18]. We note that the present results were obtained at 38 K whereas the former results as in the ref. [18] were done at the liquid nitrogen temperature. It is clear that the choice of the operating temperature of 30 K was preferable from the viewpoint of the flux creep. No remarkable difference of the relaxation rate in the trapped flux was observed in the field poles D and E, i.e., Gd123 bulk magnets with and without MP doping.

4.4. Investigation of the flux decay under AC magnetic field.

Finally, we observed the probable trapped magnetic flux decay caused by an AC magnetic field coming from the stator coils during the synchronous operation of the bulk HTS motor. The frequencies of the applied AC magnetic field from the stator were 3.33 Hz at 50 rpm and 20 Hz at 300 rpm, respectively. The average AC magnetic fields of 50 and 300 rpm operation were about 39 mT and 47 mT in r.m.s., respectively. The trapped magnetic flux of each bulk D and E was measured as shown in figure 10. Figure 10 shows the evolution of the average trapped flux as a function of the operation.

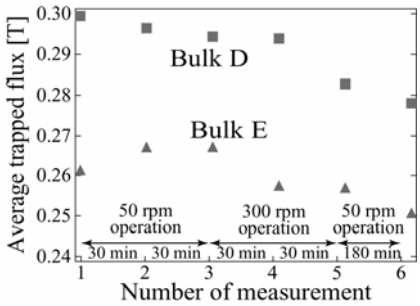

Figure 10. Evolution of the trapped magnetic field decay as a function of the varied operating conditions. The bulk E presents an increase before decreasing; this is very likely to be some measurement error.

In the case of bulk D (normal), the average trapped flux was decayed from 0.30 T to 0.28 T. On the other hand, the trapped flux decayed from 0.26 to 0.25 in the bulk E. The decay rates were 7.2 % and 4.1 % respectively. Concerning the effect of MP doping, the decayed value of the MP-doped bulk was about 30 % smaller than the normal one's.

5. Conclusion

The forthcoming HTS rotating machines provide a compact size, light weight and high output density compared to conventional machines. We adopted condensed neon gas as a cryogenic agent which was applied to a closed-cycle thermosyphon successfully. The cryo-mechanical coupling element was designed and its function is quite essential to keep low-loss refrigeration circulation in the rotating machine during operation. The increase in performances of the Gd123 bulk field poles was totally advanced. The approved J_c increase and trapped flux enhancement brought by the magnetic particles addition led to the growth of large-scale bulk field poles of 46 mm in diameter. Presently, we have reassembled the bulk-HTS motor with all the innovating advances concerning cryogenics and mechanical elements. All of these systems put together show the completion of the prototypic system of practical rotating machines such as motors or generators. Successful cooling and magnetization of the rotor field poles were obtained at 35 K in our test machine and the first-step low-output-power rotating operation was achieved up to 720 rpm. Relatively low AC losses observed in the trapped flux of the field poles at 35 K indicate that the choice of improved bulk magnets together with an improved cryo-mechanical system can lead to the practical operation of these kinds of rotating machines.

Acknowledgments

This present work has been partly supported by Fundamental Developing Association for Ship building and Offshore (REDAS) and the Iwatani Naoji Foundation (2008-2009). And this work was partially supported by KAKENHI (21360425). The authors are grateful to Hitachi Metals Co. Ltd., for providing magnetic particles.

References

[1] Zhang L, Wang S and Wang J 2009 *Physica C* **469** 685-688
[2] Nakamura T and Jung H J 2006 *Physica C* **445-448** 1115-1118
[3] Kim S B, Takano R, Nakano T, Imai M, and Hahn S Y 2009 *Physica C* **469** 1811-1815
[4] Hatzistergos M. S, Efstathiadis H, Reeves J. L, Selvamanicam V, Allen L. P, Lifshin E and Haldar P 2004 *Physica C* **405** 179-186
[5] Matsuzaki H, Kimura Y, Ohtani I, Izumi M, Ida T, Akita Y, Sugimoto H, Miki M and Kitano M 2004 *IEEE Trans. Appl. Supercond.* **15** 2222-2225
[6] Miki M, Tokura S, Hayakawa H, Inami H, Kitano M, Matsuzaki H, Kimura Y, Ohtani, I Morita E, Ogata H, Izumi M, Sugimoto H and Ida T 2006 *Supercond. Sci. Technol.***19** S494-S499
[7] Sutoh Y, Miura M, Yoshizumi M, Izumi T, Miyata S, Yamada Y and Shinohara Y 2009 *Physica C* **469** 1307-1310
[8] Xu Y, Tsuzuki K, Hara S, Zhang Y, Kimura Y and Izumi M 2009 *Phusica. C Supercond. In press*
[9] Tsuzuki K, Hara S, Xu Y, Morita M, Teshima H, Yanagisawa O, Noudem J, Harnois C and Izumi M Submitted for publication in ASC2010
[10] FINEMET® Hitachi Metals Co. Ltd.,
[11] Wimbush S C, Yu R, Bali R, Durrell J and MacManus-Driscoll J L 2009 *Physica C Supercond. In press*
[12] Sano T, Kimura Y, Sugyo D, Yamaguchi K, Matsuzaki H, Izumi M, Ida T, Sugimoto H and Miki M 2008 *J. Phys.* **97** 012194
[13] Miki M, Felder B, Tsuzuki K, Izumi M and Hayakawa H 2010 *J. Appl. Phys.* **234** 032039
[14] 2010 Tokyo University of Marine Science and Technology and Kitano Seiki Co. Ltd., *patent pending*
[15] Kimura Y, Matsuzaki H, Ohtani I, Morita E, Izumi M, Sakai N, Hirabayashi I, Miki M, Kitano M and Ida T 2006 *Supercond. Sci. Technol.* **19** S466-S471
[16] Morita E, Matsuzaki H, Kimura Y, Ogata H, Izumi M, Ida T, Murakami M, Sugimoto H and Miki M 2006 *Supercond. Sci. Technol.* **19** 1259-1263

[17] Tsuzuki K, Hara S, Xu K, Xu Y, Harnois C and Izumi M Submitted for publication in PASREG 2010
[18] Matsuzaki H, Kimura Y, Morita E, Ogata H, Ida T, Izumi M, Sugimoto H, Miki M and Kitano M 2007 *IEEE Trans. Appl. Supercond.* **17** 1553-1556